Identification of a novel microRNA-mRNA regulatory biomodule in human prostate cancer

Zhang et al. *Cell Death and Disease* (2018)9:301
DOI 10.1038/s41419-018-0293-7

Cell Death & Disease

ARTICLE Open Access

Identification of a novel microRNA-mRNA regulatory biomodule in human prostate cancer

Yanqiong Zhang[1,2], Funeng Jiang[3], Huichan He[4], Jianheng Ye[2,3], Xia Mao[1], Qiuyan Guo[1], Shu-lin Wu[2], Weide Zhong[3,4], Chin-Lee Wu[2] and Na Lin[1]

Abstract

Our recent study identified a list of differentially expressed microRNAs (miRNAs) in human prostate cancer (PCa) tissues compared to adjacent benign prostate tissues. In the current study, to identify the crucial miRNA–mRNA regulatory biomodule involved into prostate carcinogenesis based on the previous miRNA expression profile in PCa, we proposed an integrated systematic approach which combined miRNA-mediated gene expression regulatory network analysis, experimental validations in vitro and in vivo, as well as clinical significance evaluation. As a result, the CCND1-RNASEL-CDKN1A-TP73-MDM2-UBE2I axis was identified as a bottleneck in the miRNA-mediated gene expression regulatory network of PCa according to network topological analysis. The direct binding relationship between TP73 and PCa downregulated miR-193a-5p, and the direct binding relationship between UBE2I and PCa upregulated miR-188-5p were both experimentally validated. In addition, miR-193a-5p had a more significant regulatory effect on the tumor promoter isoform of TP73-deltaNp73 than on the tumor suppressive isoform of TP73-TAp73. Importantly, the deregulation of either the miR-193a-5p-TP73 or miR-188-5p-UBE2I axes was significantly associated with aggressive progression and poor prognosis in PCa patients. Gain- and loss-of-function experiments showed that miR-193a-5p efficiently inhibited in vitro PCa cell proliferation, migration, and invasion, and in vivo tumor growth, and markedly induced PCa cell apoptosis via regulating TP73 with a corresponding suppression of the CCND1-RNASEL-CDKN1A-MDM2 axis. In contrast, miR-188-5p exerted its tumor promoter roles through targeting UBE2I with a subsequent activation of the CCND1-RNASEL-CDKN1A-MDM2 axis. Taken together, this integrated analysis revealed the potential roles of the miR-193a-5p/TP73 and miR-188-5p/UBE2i negative regulation pairs in PCa. In addition to the significant clinical relevance, miR-193a-5p- and miR-188-5p-regulated CCND1-RNASEL-CDKN1A-TP73-MDM2-UBE2I signaling may be a novel regulatory biomodule in prostate carcinogenesis.

Introduction

Prostate cancer (PCa) is one of the most frequently diagnosed cancers among men and is the second leading cause of male cancer-related deaths[1]. PCa progresses in an androgen-dependent manner and responds to hormone deprivation/ablation therapy that subsequently removes circulating androgens and reduces androgen action[2]. However, many patients do not respond well to this treatment and even progress to an androgen-independent state, which is more aggressive and treatment resistant[3]. Despite an increasing use of prostate-specific antigen (PSA)-based screening for early detection of PCa at a curable stage, determining which patients

Correspondence: Weide Zhong (zhongwd2009@live.cn) or C-L. Wu (CWU2@mgh.harvard.edu) or Na Lin (nlin@icmm.ac.cn)
[1]Institute of Chinese Materia Medica, China Academy of Chinese Medical Sciences, Beijing 100700, China
[2]Department of Urology & Pathology, Massachusetts General Hospital and Harvard Medical School, Boston, MA 02114, USA
Full list of author information is available at the end of the article
These authors contributed equally: Yanqiong Zhang, Funeng Jiang, and Huichan He.
Edited by Y. Haupt

require treatment and what types of therapy should be performed remain challenging. More efficient and novel biomarkers should be identified and used to confirm the malignant potentials of PCa to predict patient clinical outcome, evaluate the risk of recurrence and select optimized therapeutic strategies.

Accumulating studies have identified multiple dysregulated microRNAs (miRNAs), which are hallmark characteristics during prostate carcinogenesis[4–6]. However, the complexity of how a single miRNA can play numerous roles in carcinogenesis, specifically in PCa, has not been fully elucidated.

Ribonuclease L (RNASEL), which is located on chromosome 1q25a, is a uniquely regulated endoribonuclease that is involved in the cleavage of viral RNA and the interferon-mediated immune response[7]. Several population-based case-control studies have investigated the associations between RNASEL variants and PCa risk[8–10]. These findings suggest that RNASEL may play a crucial role in PCa. However, little is known about the underlying molecular mechanisms through which RNASEL affects PCa.

Our recent study identified 26 differentially expressed miRNAs between PCa and adjacent benign tissues obtained from PCa patients[6]. To identify the crucial miRNAs based on this previous miRNA expression profile in PCa and their target genes and to decipher the potential relationship between the changes in the expression of these miRNAs and RNASEL, we proposed an integrated systematic approach to illustrate an miRNA-mediated gene expression regulatory network, discover crucial miRNA-target negative regulation pairs with network topological importance, validate their biological functions based on in vitro and in vivo experimental systems and evaluate their clinical significance in human PCa. A schematic diagram of this study is provided in Supplementary Figure S1.

Results

Signal axis screening of the miRNA-mediated regulatory network of PCa

Signal axis screening

In our previous study, 26 differentially expressed miRNAs, including 9 upregulated and 17 downregulated miRNAs (all fold change ≥ 1.5; $P \leq 0.05$), were identified through a comparison of PCa and adjacent benign prostate tissues[6]. Detailed information for these differentially expressed miRNAs is provided in Supplementary Table S1. The common results of three miRNA target-predicting programs (TargetScan, miRWalk, and miRanda) identified 593 candidate miRNA–mRNA pairs based on the putative interactions between differentially expressed miRNAs and target genes as well as between miRNAs and RNASEL, as shown in Supplementary Table S2. The biological significance of these miRNA–mRNA pairs is provided in Supplementary File S1—section 1 and Figure S2.

A miRNA-mediated regulatory network of PCa was constructed using the links among putative target genes of differentially expressed miRNAs and RNASEL-upstream miRNAs. This network contained 243 nodes and 1167 edges (Supplementary Table S3). Following the calculation of four topological features, including 'Degree,' 'Node betweenness' and 'Closeness' and 'K coreness,' 89 hubs with topological importance were chosen, and the hub network was also constructed based on the direct interactions among hubs. Detailed information about the topological features of the hubs is provided in Supplementary Table S4.

Because genes with close interconnections are often involved in the same functional modules or pathways, modularity may be another important aspect of an interaction network. In the current study, we performed modularity analysis using the Markov clustering algorithm and divided the above-mentioned hub network into the following three functional modules: 'Cell cycle, Pathways in cancer, and P53 signaling pathway' (48 nodes); 'MAPK signaling pathway and Focal adhesion' (38 nodes); and 'VEGF signaling pathway' (3 nodes) (Supplementary Figure S3).

Moreover, the 'Edge-betweenness' of each interaction in the hub network was calculated because an interaction with a high 'Edge-betweenness' is defined as a bottleneck that has many 'shortest paths' going through it and controls the rate of information flow. As shown in Supplementary Table S5, the interaction between CCND1-CDKN1A had the highest 'Edge-betweenness' value (40.10), implying its importance in connecting different functional modules within the network.

Among the putative targets of differentially expressed miRNAs in PCa, TP73 was a putative target of miR-193a-5p (PCa-downregulated miRNA, Supplementary Table S1) and interacted with CDKN1A. Additionally, UBE2I was a putative target of miR-188-5p (PCa-upregulated miRNA, Supplementary Table S1) and interacted with TP73 and CDKN1A through MDM2 (Fig. 1a). Moreover, we also found 17 miRNAs that act upstream of RNASEL and were shared with CCND1 and/or CDKN1A, implying similar functions among the three genes (Fig. 1a). Thus, we hypothesized that the signal axis of CCND1-RNASEL-CDKN1A-TP73-MDM2-UBE2I might play a crucial role in the miRNA-mediated regulatory network of human PCa.

Biological significance of the CCND1-RNASEL-CDKN1A-TP73-MDM2-UBE2I signal axis

Cyclin D1 (CCND1) is amplified and overexpressed in a variety of human malignancies, including human PCa[11,12].

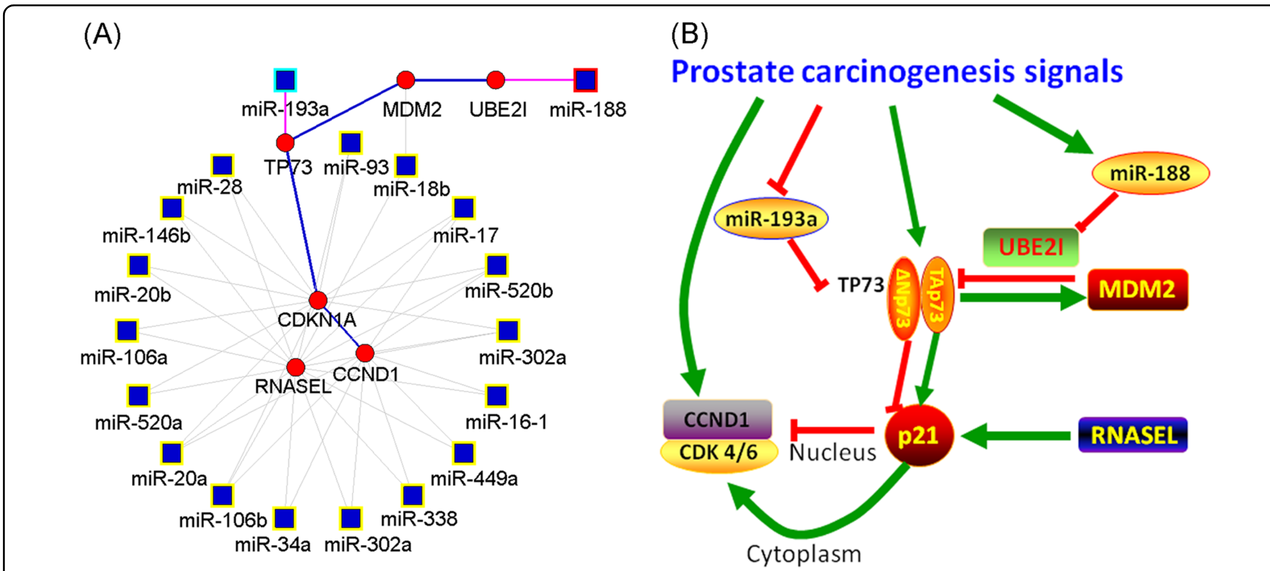

Fig. 1 Involvement of the miR-193a-5p and miR-188-5p-regulated CCND1-RNASEL-CDKN1A-TP73-MDM2-UBE2I signal axis in prostate cancer (PCa) cells. a Sub-network of the CCND1-RNASEL-CDKN1A-TP73-MDM2-UBE2I signal axis and the corresponding upstream microRNAs. Nodes with a red border refer to an upregulated microRNA in PCa. Nodes with a blue border refer to a downregulated microRNA in PCa. Nodes with a yellow border refer to common microRNAs upstream of CCND1, RNASEL and CDKN1A. **b** Molecular model of the miR-193a-5p and miR-188-5p-regulated CCND1-RNASEL-CDKN1A-TP73-MDM2-UBE2I signal axis in PCa cells

In accordance with the androgen dependence of PCa, CCND1 interacts with the androgen signaling pathway, suggesting that androgens may indirectly stimulate cell growth via regulating the expression of cell cycle-associated genes[13].

CDKN1A (also called p21), which is a CDK inhibitor (CKI), can suppress the effects of the CCND1-CDK4 complex in the G1 phase, leading to G1 arrest. Importantly, p21 activation requires high levels of tumor protein p73 (TP73)[14].

TP73 encodes a variety of protein isoforms with opposing functions via alternative promoters at the 5′-end or differential splicing at the 3′-end[15,16]. Among the isoforms, TAp73 variants, which contain the NH2-terminal transactivation domain, are tumor suppressors and mimic TP53 function in experimental systems. In contrast, deltaNp73 variants, which are transactivation-deficient isoforms, function as oncogenes and cannot induce apoptosis and cell cycle arrest because they are direct competitors for the DNA-binding sites and/or they form hetero-duplexes with TP53 and the transactivation-competent TAp73 variants[17]. Hence, the biological functions of miRNAs that directly target TP73 may depend on which isoforms they mainly regulate. Moreover, Guan et al.[18] observed a significant increase of deltaNp73 in PCa tissues compared with benign prostate hyperplasia tissues and confirmed that the incidence of positive expression of deltaNp73 is correlated with the Gleason score in PCa.

RNASEL regulates p21-mediated G1 growth arrest in an AU-rich element-dependent manner. Overexpression of RNASEL may activate p21[19].

Ubiquitin-conjugating enzyme E2 I (UBE2I) encodes a member of the E2 ubiquitin-conjugating enzyme family (UBC9), which may modify proteins with ubiquitin, a crucial cellular mechanism for targeting abnormal or short-lived proteins for degradation. A previous study based on a yeast two-hybrid system found that RAD52-dependent processes, cell cycle control, p53-mediated pathway(s), and ubiquitination interact through human UBE2I[20].

We illustrated a model to hypothesize the involvement of the miR-193a-5p-regulated and miR-188-5p-regulated CCND1-RNASEL-CDKN1A-TP73-MDM2-UBE2I signal axis in prostate carcinogenesis (Fig. 1b). In PCa tissues, the increased expression of miR-188-5p may negatively regulate the expression of its candidate target gene, UBE2I, which may reduce the degradation of TP73. Simultaneously, the downregulation of miR-193a-5p in PCa tissues might result in the upregulation of TP73. Because there are different isoforms of TP73 with varying potential for tumor progression, TP73 may play opposite roles depending on changes in the TAp73/ deltaNp73 isoform ratio. If the TAp73/deltaNp73 isoform ratio is increased by miR-193a-5p in PCa cells, the expression levels of MDM2 and P21 (CDKN1A) might be elevated, and TP73 might function as a tumor suppressor, leading to the reduced effect of the CCND1/CDK4 complex and

Table 1 Association of two miRNA–mRNA pairs with clinicopathologic features of prostate cancer patients based on TCGA data

Clinical features	Case No.[a]	miR-193a-low		TP73-high		miR-193a-low/ TP73-high		miR-188-high		UBE2I-low		miR-188-high/UBE2I-low	
		(*n*, %)	*P*	(*n*, %)	*P*	(*n*, %)	*P*	(*n*, %)	*P*	(*n*, %)	*P*	(*n*, %)	*P*
Age (years)													
<55	83	18 (21.7)	0.883	56 (67.5)	0.265	13 (37.1)	0.422	40 (48.2)	0.698	38 (45.8)	0.162	19 (43.3)	0.405
>55	406	85 (20.9)		245(60.3)		53 (29.1)		204 (50.2)		206 (50.7)		101 (51.3)	
Biochemical-recurrence status													
Negative	365	78 (21.4)	0.499	227 (62.2)	1.000	48 (30.8)	0.516	160 (43.8)	0.033	167 (45.8)	0.035	79 (45.9)	1.000
Positive	59	15 (25.4)		37 (62.7)		11 (37.9)		40 (67.8)		40 (67.8)		14 (46.7)	
Gleason pattern (Primary)													
Grade 3	191	34 (17.8)	0.310	120 (62.8)	0.114	20 (26.0)	0.275	78 (40.8)	0.018	98 (51.3)	0.100	44 (44.4)	<0.001
Grade 4	248	59 (23.8)		144 (58.1)		36 (30.8)		129 (52.0)		116 (46.8)		60 (48.0)	
Grade 5	49	10 (20.4)		36 (73.5)		10 (43.5)		38 (77.6)		30 (61.2)		16 (100.0)	
T-stage													
<T2	176	30 (17.0)	0.210	105 (59.7)	0.299	16 (21.9)	0.047	87 (49.4)	0.386	75 (42.6)	0.003	39 (42.4)	0.007
>T2	226	51 (22.6)		147 (65.0)		39 (36.8)		113 (50.0)		140 (61.9)		69(62.2)	
N-stage													
N0	339	71 (20.9)	0.545	207 (61.1)	0.798	44 (29.5)	0.342	168 (49.6)	0.882	165 (48.7)	0.061	72 (43.6)	<0.001
N1	79	19 (24.1)		50 (63.3)		15 (37.5)		40 (50.6)		46 (58.2)		28(82.4)	
Disease-free status													
Free	392	79 (20.2)	0.318	233 (59.4)	0.042	48 (27.3)	0.031	189 (48.2)	0.562	188 (48.0)	0.052	89 (46.6)	0.038
Recurred/progressed	91	23 (25.3)		65 (71.4)		17 (45.9)		52 (57.1)		56 (61.5)		32 (64.0)	

[a] Some clinical features lack the information, so the total numbers according to various features are different

G1 arrest. If the TAp73/deltaNp73 isoform ratio is decreased by miR-193a-5p in PCa cells, the expression levels of MDM2 and P21 (CDKN1A) might be reduced, and TP73 might function as an oncogene. Taken together, an imbalance of the miR-193a-5p- and miR-188-5p-regulated CCND1-RNASEL-CDKN1A-TP73-MDM2-UBE2I biomodule might be involved in prostate carcinogenesis.

Deregulation of miR-193a-5p-TP73 and miR-188-5p-UBE2I pairs associated with aggressive progression and poor prognosis in PCa patients

To evaluate the associations of miR-193a-5p-TP73 and miR-188-5p-UBE2I expression with various clinicopathological features of PCa patients, the optimal cutoff points of miR-193a-5p, TP73, miR-188-5p and UBE2I expression were screened. The optimal cutoff point was defined with regard to the miRNA/mRNA expression level either alone or in combination with the most significant BCR-free survival. Using the optimal cutoff points, 490 PCa patients were divided into miR-193a-5p-high/low, TP73-high/low, miR-188-5p-high/low and UBE2I-high/low groups. As shown in Table 1, high TP73 expression was significantly associated with disease-free status ($P = 0.042$), and low miR-193a expression combined with high TP73 expression frequently occurred in PCa patients with advanced T-stage ($P = 0.047$) and positive disease recurrence ($P = 0.031$). In addition, PCa patients with high miR-188-5p or low UEB2I expression had a higher incidence of biochemical recurrence than those with low miR-188-5p or high UBE2I expression (both $P < 0.05$). Gleason grades of PCa patients with high miR-188-5p expression and miR-188-5p-high/UBE2I-low expression were significantly higher than those of patients with low miR-188-5p expression and miR-188-5p-low/UBE2I-high expression, respectively (both $P < 0.05$). Both low UBE2I expression and combined miR-188-5p-high/UBE2I-low expression were significantly associated with advanced T stage (both $P < 0.05$). PCa patients with miR-188-5p-high/UBE2I-low expression frequently experienced advanced N stage and recurred/progressed disease status (both $P < 0.05$, Table 1).

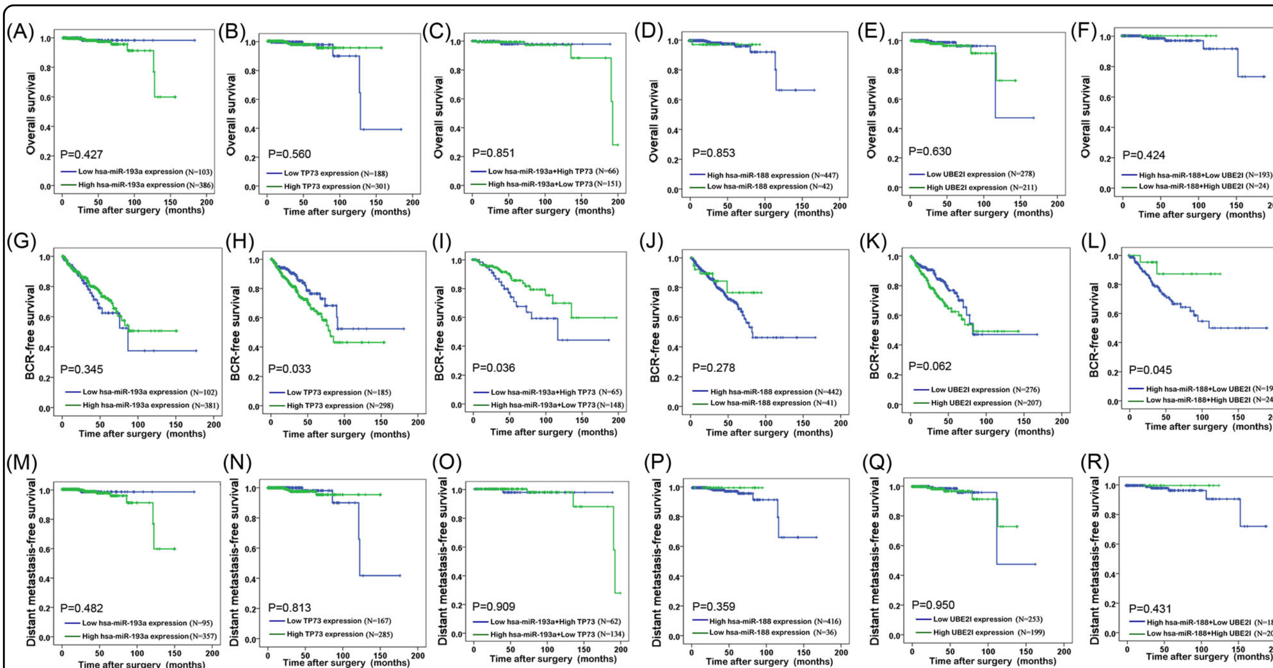

Fig. 2 Overall survival (**a–f**), biochemical recurrence (BCR)-free survival (**g–l**) and distant-metastasis-free survival (**m–r**) curves based on miR-193a and/or TP73 as well as miR-188 and/or UBE2I expression in patients with prostate cancer based on TCGA data

The prognostic values of miR-193a-5p and/or TP73 expression as well as miR-188-5p and/or UBE2I expression in PCa patients were evaluated using the Kaplan–Meier method based on TCGA data. As shown in Fig. 2h, i, high TP73 expression alone or in combination with low miR-193a expression were both significantly associated with short BCR-free survival when compared with low TP73 expression ($P = 0.036$) and miR-193a-5p-high /TP73-low expression ($P = 0.033$) groups, respectively. Moreover, only miR-188-5p-high/UBE2I-low expression was significantly associated with short BCR-free survival ($P = 0.045$, log-rank test, Fig. 2l). There were no significant prognostic values of miR-193a-5p/TP73 and miR-188-5p/UBE2I axes in overall and disease metastasis-free survivals (Fig. 2a–f and Fig. 2m–r).

TP73 and UBE2I are respective direct targets of miR-193a-5p and miR-188-5p in PCa cells

The results shown in Supplementary Figure S4A indicated that the endogenous expression of TP73 in PCa cells and in established tumors associated with LNCaP cells stably expressing miR-193a-5p was significantly reduced at both the mRNA and protein levels. In contrast, knockdown of miR-193a-5p by its inhibitor efficiently increased the expression of TP73 mRNA and protein in both PCa cells and established tumors (Supplementary Figure S4A). The findings for the miR-188-5p/UBE2I pair were similar to those for the miR-193a-5p/TP73 pair (Supplementary Figure S4B). Because TP73 has various isoforms with opposing functions, we performed qRT-PCR to evaluate the regulatory effects of miR-193a-5p on a tumor promoter isoform of TP73 (deltaNp73) and a tumor suppressive isoform of TP73 (TAp73). As shown in Supplementary Figure S5, the enforced expression of miR-193a-5p in PCa cells effectively reduced the expression of deltaNp73 mRNA and increased the ratio of TAp73 to deltaNp73. In contrast, the suppression of miR-193a-5p upregulated the expression of deltaNp73 mRNA and decreased the ratio of TAp73 to deltaNp73. These results suggest a more significant regulatory effect of miR-193a-5p on deltaNp73 than on TAp73.

To verify whether TP73 was a direct target of miR-193a-5p, and UBE2I was a direct target of miR-188-5p, a luciferase reporter containing the complimentary seed sequences of miR-193a-5p/miR-188-5p at the 3′-UTR region of TP73 (Transcript NM_001126242, protein name: deltaNp73 gamma) /UBE2I (Transcript NM_003345) mRNA was constructed. At 48 h after transfection, luciferase activity of the TP73 reporter was significantly reduced by co-transfection with miR-193a-5p mimics. In contrast, the luciferase activity of the TP73 reporter containing the mutated sequence of the same fragment was not affected by co-transfection with miR-193a-5p mimics (Supplementary Figure S6A). These findings were similar with those for the miR-188-5p/UBE2I pair (Supplementary Figure S6B).

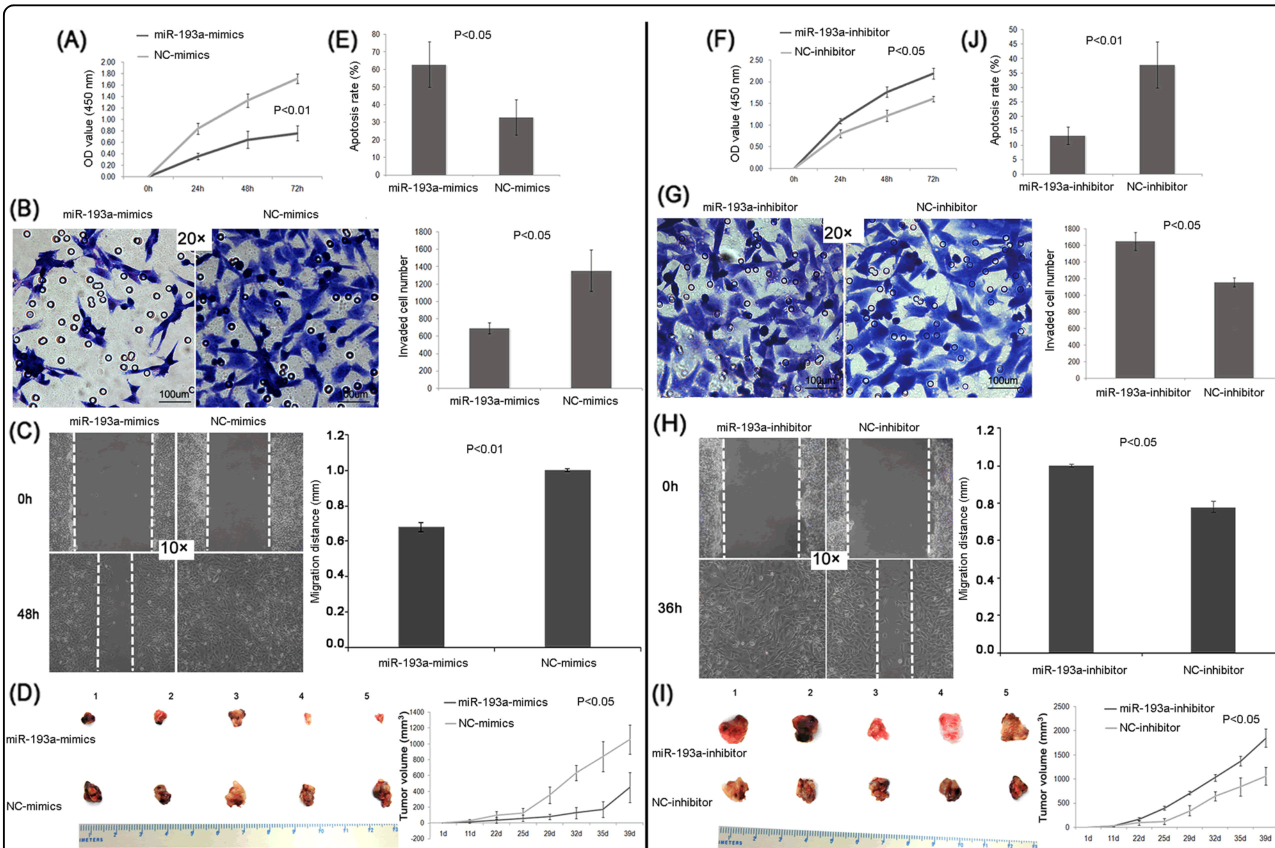

Fig. 3 miR-193a-5p inhibits LNCaP cell proliferation, migration and invasion and in vivo tumor growth, but it induces LNCaP cell apoptosis. a The CCK-8 assay indicated that proliferation of LNCaP cells transfected with miR-193a-5p mimics was significantly reduced compared with that of cells transfected with the negative control. **b** The transwell assay showed that the enforced expression of miR-193a-5p significantly reduced the invasive activities of LNCaP cells compared with those of control cells. **c** The wound-healing assay revealed that miR-193a-5p overexpression efficiently weakened the migratory ability of LNCaP cells. **d** Based on the in vivo system, LNCaP cells stably expressing miR-193a-5p formed significantly smaller tumor nodules and showed markedly slow growth of tumor xenografts compared with the controls. **e** The apoptotic rate of LNCaP cells with miR-193a-5p upregulation was significantly higher than that of control cells. **f–j** Knockdown of miR-193a-5p expression with the corresponding inhibitor efficiently enhanced the cellular proliferation, invasion ability and motility of LNCaP cell lines and promoted the growth of tumor xenografts, but it reduced cellular apoptosis in vitro. Note: '×10' and '×20' refer to the magnification

The above data suggest that TP73 and UBE2I may be direct targets of miR-193a-5p and miR-188-5p, respectively, in PCa cells.

miR-193a-5p functions as a tumor suppressor in PCa via targeting TP73

CCK-8 assays indicated that proliferation rate of LNCaP and PC3 cells transfected with miR-193a-5p mimics was significantly lower than those transfected with the negative control (Fig. 3a and Supplementary Figure S7A). Transwell assays showed that the enforced expression of miR-193a-5p significantly reduced the invasive activities of both LNCaP and PC3 cells (Fig. 3b and Supplementary Figure S7B). Wound-healing assays also revealed that miR-193a-5p overexpression efficiently weakened the migratory abilities of both LNCaP and PC3 cells (Fig. 3c and Supplementary Figure S7C). Based on the in vivo system, we found that the LNCaP cells stably expressing miR-193a-5p formed significantly smaller tumor nodules and showed markedly slow growth of tumor xenografts (Fig. 3d). In contrast, the apoptotic rates of LNCaP and PC3 cells with miR-193a-5p upregulation were significantly higher than those of control cells (Fig. 3e and Supplementary Figure S7D). Interestingly, knockdown of miR-193a-5p expression by the corresponding inhibitor efficiently enhanced the cellular proliferation, invasion ability and motility of PCa cells and promoted the growth of tumor xenografts; it reduced cellular apoptosis in vitro (Fig. 3f–j and Supplementary Figure S7E–H).

To determine the roles of TP73 in biological functions of miR-193a-5p, pCDNA3.1(+) vectors expressing TP73 without its 3′-UTR (using the binding site of 3′UTR of

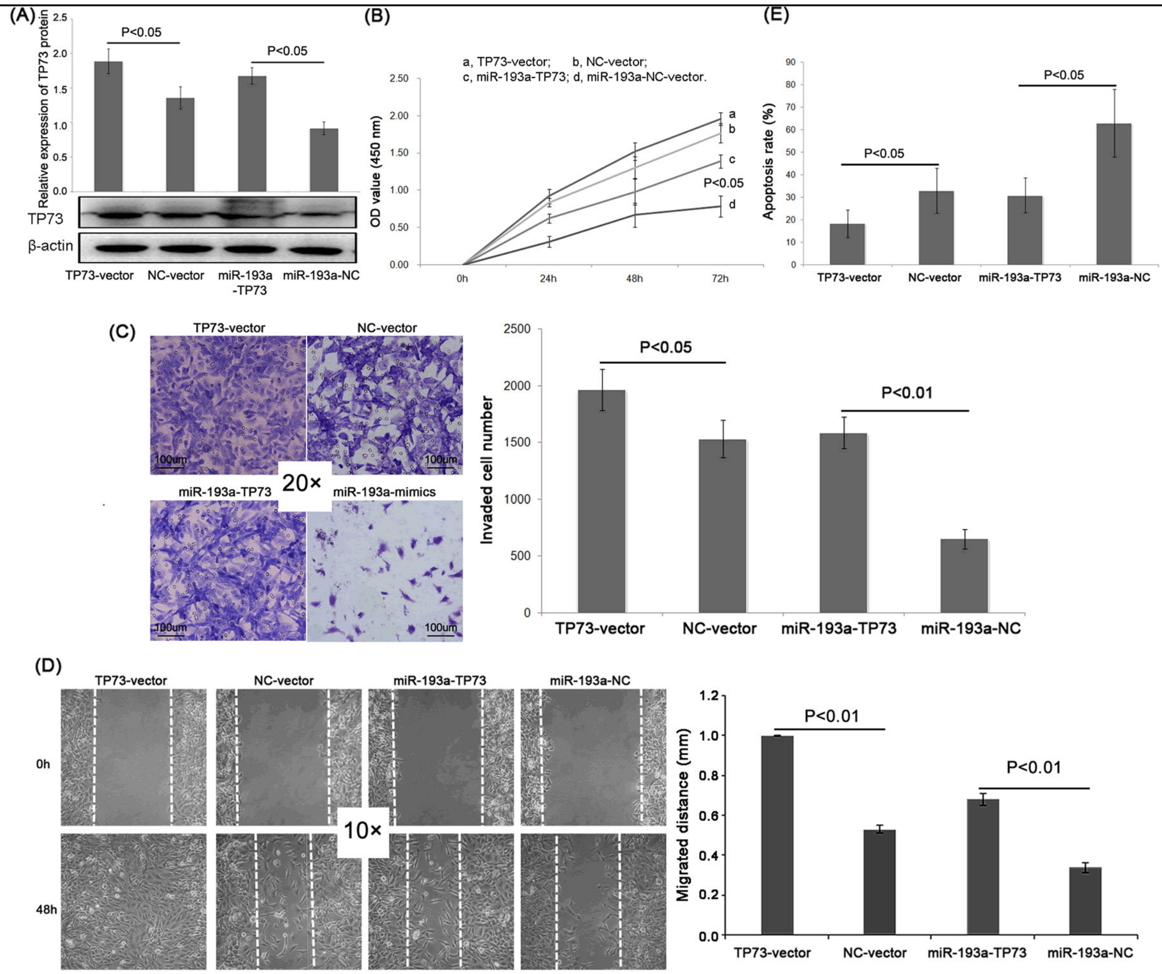

Fig. 4 Re-expression of TP73 rescues the tumor suppressive effects of miR-193a-5p in LNCaP cells. a Endogenous TP73 protein expression levels were detected by western blotting in LNCaP cells transfected with the miR-193a-5p mimic in the presence of TP73 or vector control for 48 h. **b–e** Expression of TP73 using a construct lacking its 3′-UTR rescued the biological effects associated with re-introduction of miR-193a-5p, as indicated by cell invasion, viability, migration and apoptosis assays. These experiments were performed after transfection of miR-193a-5p mimics and/or the TP73 3′-UTR (–) for 48 h. The data are representative of at least three independent experiments and are presented as the mean ± s.e.m. Note: '×10' and '×20' refer to the magnification

Transcript NM_001126242, the protein name of which is deltaNp73 gamma) were generated. As shown in Fig. 4a and Supplementary Figure S8A, the endogenous expression of TP73 protein in LNCaP and PC3 cells transfected with miR-193a-5p mimics in the presence of pCDNA3.1-TP73 was significantly higher than that in cells transfected with miR-193a-5p and vector control. In vitro cellular proliferation (Fig. 4b and Supplementary Figure S8B), invasion (Fig. 4c and Supplementary Figure S8C), migration (Fig. 4d and Supplementary Figure S8D) and apoptosis (Fig. 4e and Supplementary Figure S8E) all indicated that restoration of TP73 expression dramatically attenuated the effects induced by miR-193a-5p.

These findings suggest that the tumor suppressive roles of miR-193a-5p may be mediated by inhibiting its target gene, TP73.

miR-188-5p functions as an onco-miRNA in PCa by targeting UBE2I

CCK-8 assays indicated that proliferation rates of LNCaP and PC3 cells were significantly increased by transfection with miR-188-5p mimics (Fig. 5a and Supplementary Figure S9A). Transwell and wound-healing assays showed that the enforced expression of miR-188-5p dramatically enhanced the invasive and migratory activities, respectively, of both LNCaP and PC3 cells (Figure 5b, c and Supplementary Figure S9B, C). Based on the in vivo system, miR-188-5p overexpression promoted tumor growth (Fig. 5d). In contrast, the apoptotic rates of LNCaP and PC3 cells with miR-188-5p upregulation were significantly lower than those of control cells (Fig. 5e and Supplementary Figure S9D). Interestingly, knockdown of miR-188-5p expression by the corresponding inhibitor

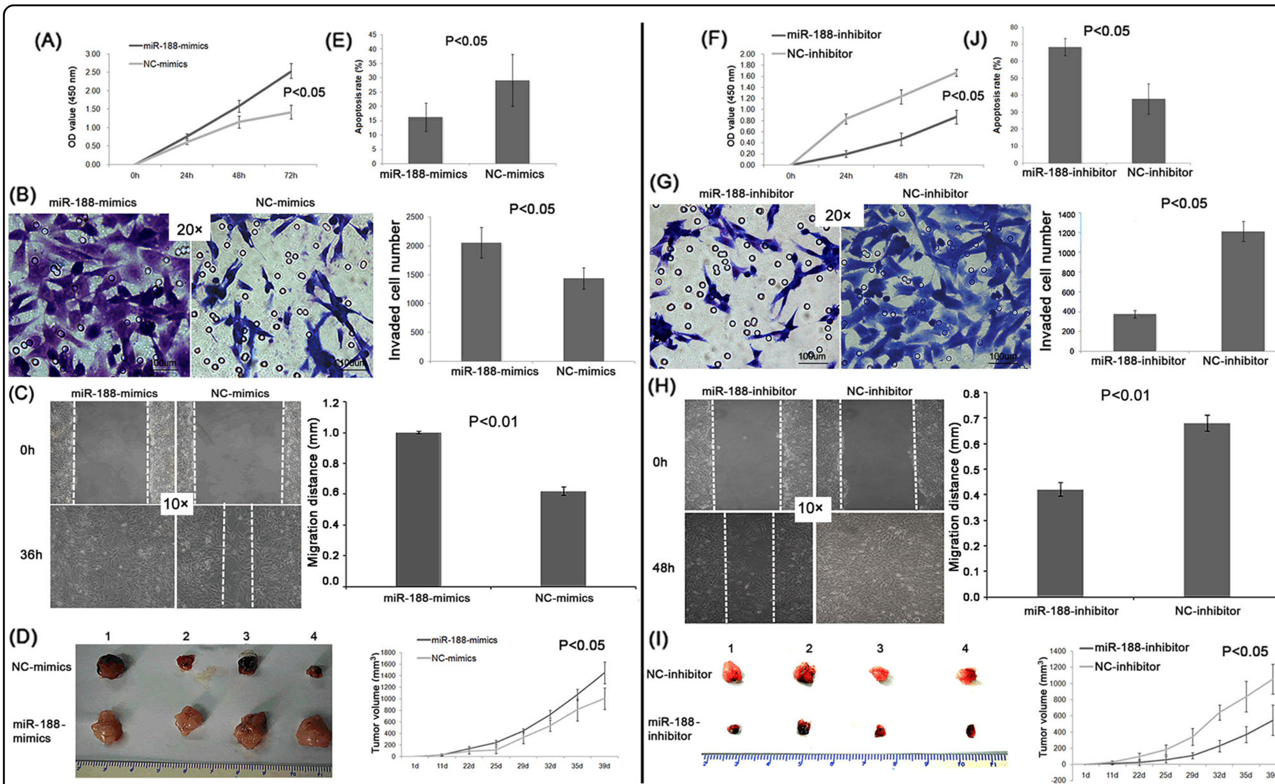

Fig. 5 miR-188-5p promotes LNCaP cell proliferation, migration and invasion and in vivo tumor growth, but it suppresses LNCaP cell apoptosis. a The CCK-8 assay indicated that the proliferation of LNCaP cells transfected with miR-188-5p mimics was significantly greater than that of cells transfected with the negative control. **b** The transwell assay showed that the enforced expression of miR-188-5p significantly enhanced the invasive activities of LNCaP cells compared with those of control cells. **c** The wound-healing assay revealed that miR-188-5p overexpression efficiently enhanced the migratory ability of LNCaP cells. **d** The apoptotic rate of LNCaP cells with miR-188-5p upregulation was significantly lower than that of control cells. **e–h** Knockdown of miR-188-5p expression by the corresponding inhibitor efficiently weakened the cellular proliferation, invasion ability and motility of LNCaP cell lines and inhibited the growth of tumor xenografts, but it enhanced cellular apoptosis qin vitro. Note: '×10' and '×20' refer to the magnification

reduced the enhanced effects on cellular proliferation, invasion and motility of PCa cell lines and the growth of tumor xenografts, but it increased cellular apoptosis in vitro (Fig. 5f–j and Supplementary Figure S9E–H).

In the rescue experiments, the endogenous expression of UBE2I protein in LNCaP and PC3 cells transfected with miR-188-5p mimics in the presence of pCDNA3.1-UBE2I was significantly higher than that in cells transfected with miR-188-5p and vector control (Fig. 6a and Supplementary Figure S10A). In vitro cellular proliferation (Fig. 6b and Supplementary Figure S10B), invasion (Fig. 6c and Supplementary Figure S10C), migration (Fig. 6d and Supplementary Figure S10D), and apoptosis (Fig. 6e and Supplementary Figure S10E) all indicated that restoration of UBE2I expression dramatically attenuated the effects induced by miR-188-5p.

These findings suggest that the onco-miRNA roles of miR-188-5p may be mediated by inhibiting its target gene, UBE2I.

CCND1, RNASEL, CDKN1A, and MDM2 function as the downstream effectors of the miR-193a-5p-TP73 and miR-188-5p-UBE2I axes

According to our above-mentioned network analysis, the CCND1-RNASEL-CDKN1A-TP73-MDM2-UBE2I axis may play crucial roles in the imbalanced miRNA-mediated regulatory network of human PCa. After validation of the clinical significance and the biological functions of the miR-193a-5p-TP73 and miR-188-5p-UBE2I axes, we investigated their regulatory effects on the protein expression levels of CCND1, RNASEL, CDKN1A, and MDM2 by western blot analysis. As shown in Fig. 7a and b, the enforced expression of miR-193a-5p in two PCa cell lines, LNCaP and PC3, significantly reduced the protein expression levels of TP73, CCND1 and MDM2 but increased the protein expression levels of RNASEL and CDKN1A (all $P < 0.05$). In contrast, miR-188-5p overexpression markedly increased the protein expression levels of CCND1 and MDM2 but

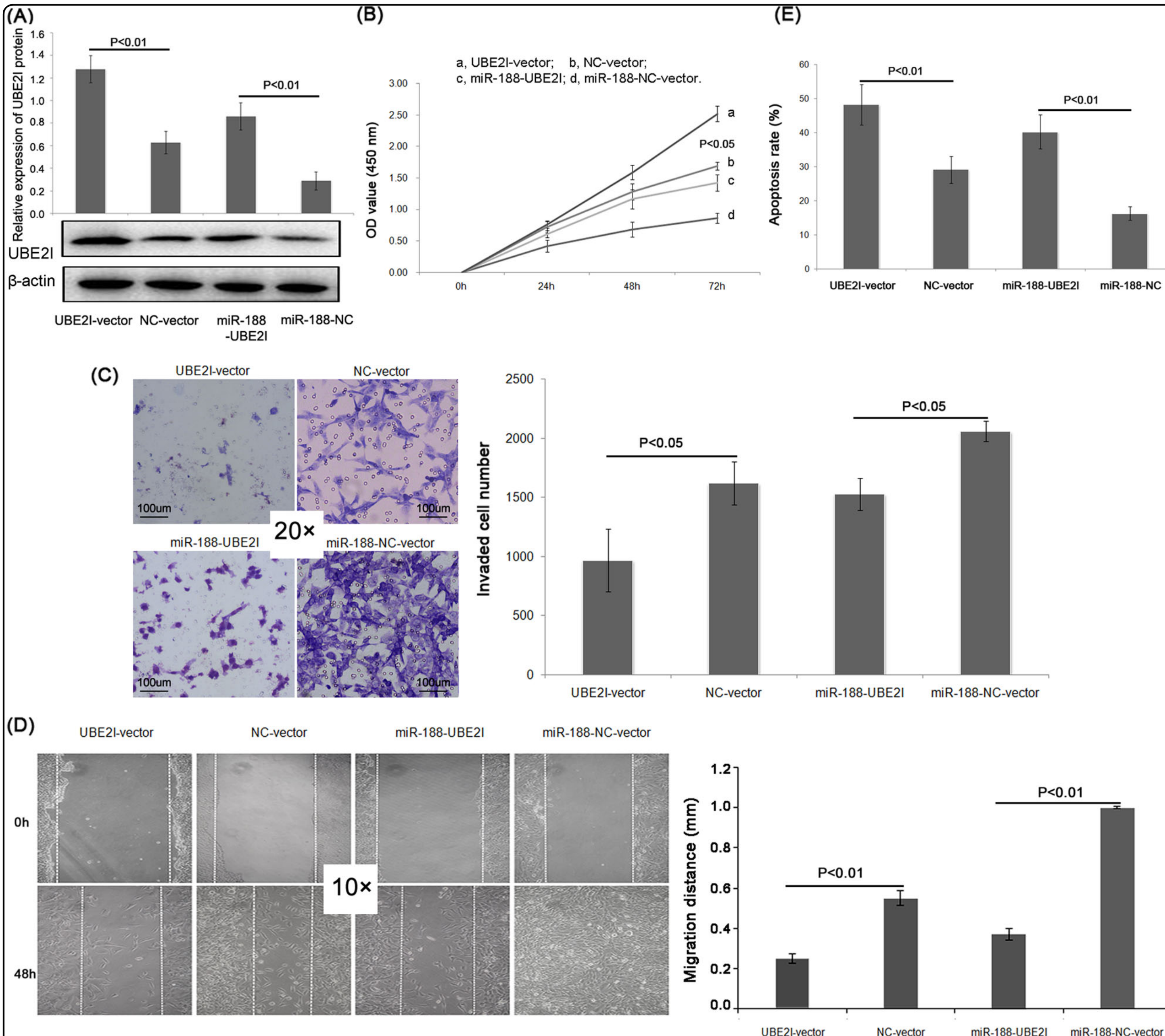

Fig. 6 Re-expression of UBE2I rescues the oncogenic effects of miR-188-5p in LNCaP cells. a Endogenous UBE2I protein expression levels were detected by western blotting in LNCaP cells transfected with the miR-188-5p mimic in the presence of UBE2I or vector control for 48 h. **b–e** Expression of UBE2I using a construct lacking its 3′-UTR rescued the biological effects associated with re-introduction of miR-188-5p, as indicated by cell invasion, viability, migration and apoptosis assays. These experiments were performed after co-transfection of miR-188-5p mimics and/or the UBE2I 3′-UTR (–) for 48 h. The data are representative of at least three independent experiments and are presented as the mean ± s.e.m. Note: '×10' and '×20' refer to the magnification

decreased the protein expression levels of UBE2I, RNASEL and CDKN1A (all $P < 0.05$). In addition, the expression levels of CCND1 and MDM2 proteins were dramatically upregulated, but the expression levels of RNASEL and CDKN1A proteins were significantly downregulated, in LNCaP and PC3 cells with the overexpression of TP73 (all $P < 0.05$, Fig. 7c), which were opposite to the miR-193a-5p enforced cells. Moreover, the enforced expression of UBE2I in two PCa cell lines markedly reduced the protein expression levels of CCND1 and MDM2 but increased the protein expression levels of RNASEL and CDKN1A (all $P < 0.05$, Fig. 7d), which were also opposite to the miR-188-5p enforced cells as mentioned above. Furthermore, the qPCR analysis shown in Supplementary Figure S11 also indicated the similar results to the western blot as mentioned above (Fig. 7). These findings suggest that CCND1, RNASEL, CDKN1A, and MDM2 may function as the downstream effectors of the miR-193a-5p-TP73 and miR-188-5p-UBE2I axes.

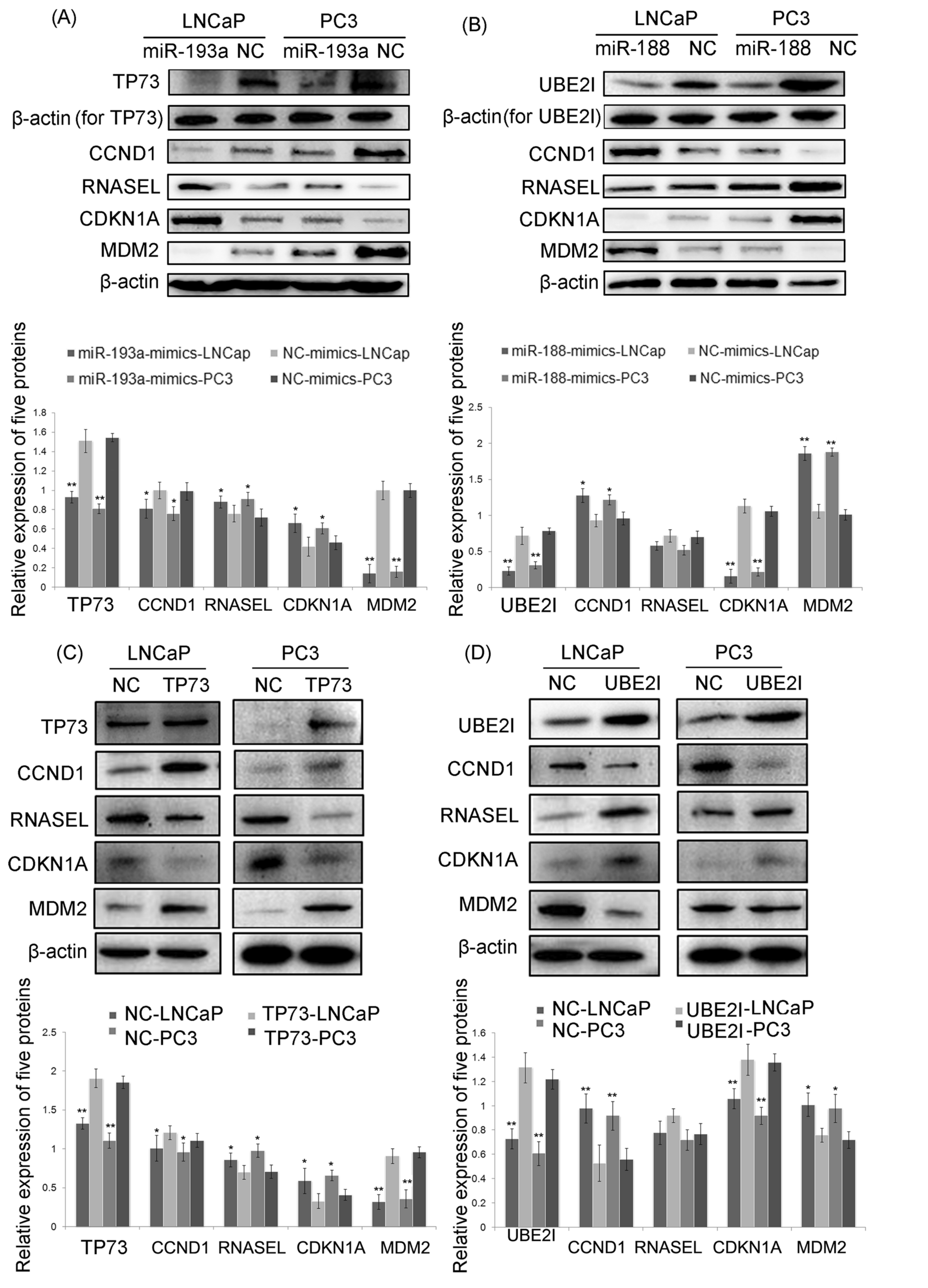

Fig. 7 (See legend on next page.)

(see figure on previous page)

Fig. 7 Western blot analysis indicated that CCND1, RNASEL, CDKN1A and MDM2 function as the downstream effectors of the miR-193a-TP73 and miR-188-UBE2I axes at a protein level. **a** Relative protein expression levels of TP73, CCND1, RNASEL, CDKN1A, and MDM2 in LNCaP and PC3 cells transfected with miR-193a/NC-mimics. **b** Relative protein expression levels of UBE2I, CCND1, RNASEL, CDKN1A, and MDM2 in LNCaP and PC3 cells transfected with miR-188/NC-mimics. **c** Relative protein expression levels of TP73, CCND1, RNASEL, CDKN1A, and MDM2 in LNCaP and PC3 cells transfected with TP73/NC-expression vector. **d** Relative protein expression levels of UBE2I, CCND1, RNASEL, CDKN1A, and MDM2 in LNCaP and PC3 cells transfected with UBE2I/NC-expression vector. The data are representative of at least three independent experiments and are presented as the mean ± s.e.m. *$P < 0.05$, compared with the normal control group; **$P < 0.01$, compared with the normal control group

Discussion

miRNA dysregulation is a hallmark characteristic during prostate carcinogenesis. However, the underlying mechanisms of the miRNA-regulated oncogenic biomodules in PCa have not been fully elucidated. Previously, we identified a list of aberrantly expressed miRNAs based on a clinical cohort of PCa patients using an miRNA microarray approach. In this study, we constructed an miRNA-mediated gene expression regulatory network of PCa and identified a novel miRNA–mRNA regulatory biomodule of miR-193a-5p- and miR-188-5p-regulated CCND1-RNASEL-CDKN1A-TP73-MDM2-UBE2I signaling. Following network topological analysis, clinical significance evaluation and a series of functional experimental validations, we demonstrated that an imbalance in this biomodule may be implicated in prostate carcinogenesis, progression and patient prognosis.

Accumulating studies have reported the downregulation of miR-193a in various human cancers and revealed its involvement in carcinogenesis and cancer progression[21–25]. Similarly, our clinical analysis showed that dysregulation of the miR-193a/TP73 axis was closely correlated with advanced T-stage and positive disease recurrence. In addition, the BCR-free survival of PCa patients with miR-193a-5p-low/TP73-high expression was shorter than that of patients with miR-193a-5p-high/TP73-low expression. Functional experiments identified TP73 as a target gene of miR-193a-5p and confirmed the TP73-mediated tumor suppressive roles of the miR-193a-5p/TP73 axis in malignant PCa cell lines. More interestingly, Jacques et al.[25] found that miR-193a-5p controls Cisplatin chemoresistance in primary bone tumors via TAp73β. However, our data showed a more significant regulatory effect of miR-193a-5p on deltaNp73 (a tumor promoter isoform of TP73) than on TAp73 (a tumor suppressive isoform of TP73), implying different regulatory mechanisms of miR-193a-5p across cancer types.

miR-188, a cancer-related miRNA, functions as a tumor suppressor in oral squamous cell carcinoma[26] and hepatocellular carcinoma[27]. Notably, Zhang et al.[28] suggested that miR-188-5p might exert tumor suppressor functions in the carcinogenesis of PCa, which disagrees with our findings. The reasons for this discrepancy might are explained below. First, the microarray data showing the marked upregulation of miR-188-5p in PCa tissues compared with adjacent non-cancerous prostate tissues were based on clinical samples. In contrast, Zhang's miRNA array data displaying the decreased expression of miR-188-5p were obtained from paired metastatic LTL-313H and non-metastatic LTL-313B PCa xenografts. Second, the TCGA data set used in our statistical analysis included 490 PCa samples, which is greater than the sample number in Zhang's clinical cohort ($n = 180$). Using this larger data set, we demonstrated that high-miR-188-5p and/or low-UBE2I expression was significantly associated with aggressive PCa progression and poor patient prognosis. Third, both groups used the same PCa cell lines (PC3 and LNCaP) to perform a series of in vitro and in vivo functional experiments. However, different findings were obtained, which may be due to the heterogeneity of cancer cells in different experimental platforms. Therefore, further large-scale validations are needed in the future.

We also determined the downstream effectors of the miR-193a-5p/TP73 and miR-188-5p/UBE2i axes. CCND1-RNASEL-CDKN1A-TP73-MDM2-UBE2I signaling was identified as a bottleneck in the miRNA-mediated gene expression regulatory network of PCa, which represents key interactions with surprising functional and dynamic properties[29]. Based on the molecular interactions and the implications of this signaling in cancer[11–20,30], we illustrated a biomodule of miR-193a-5p- and miR-188-5p-regulated CCND1-RNASEL-CDKN1A-TP73-MDM2-UBE2I signaling in Fig. 1b. Our experimental validations further confirmed the regulatory effects of miR-193a-5p and miR-188-5p on this signaling axis at both mRNA and protein levels.

Collectively, this integrated analysis of an miRNA-mediated gene expression regulatory network reveals the potential roles of miR-193a-5p/TP73 and miR-188-5p/UBE2i negative regulation pairs in PCa. Our data showed that miR-193a-5p and miR-188-5p targeted TP73 and UBE2I respectively at mRNA and protein level, suggesting that the two miRNAs may not work at the translational level throughout a DICER mechanism. In addition to the significant clinical relevance, miR-193a-5p- and miR-188-5p-regulated CCND1-RNASEL-CDKN1A-TP73-MDM2-UBE2I signaling may be a novel regulatory biomodule within prostate carcinogenesis. However, there are several limitations in the clinical cohort using in this study. For example, only 71 in 490 (14.5%) PCa patients occurred BCR; Only 10 in 490 (2.0%) patients died of PCa during the follow-up of overall survival. The imbalance of the feature distribution in this TCGA cohort might lead to the minor clinical relevance of the two miRNA/target pairs. Therefore, further prognostic evaluation based on other independent and large cohorts in compliance with statistical standard are required.

Methods

miRNA-mediated gene expression regulatory network analysis

A miRNA-mediated gene expression regulatory network was constructed based on the links between miRNAs and the corresponding putative target genes and the interactions among the putative target genes (Supplementary File S1—sections 2–4).

Four topological features of nodes, including 'Degree,' 'Node betweenness,' 'Closeness' and 'K coreness,' and one topological feature of edges (links among nodes), namely, 'Edge betweenness,' were calculated to assess the topological importance of nodes and edges in the miRNA-mediated gene expression regulatory network. Each feature mentioned above is defined in Supplementary File S1—section 5.

In addition, functional modularity was analyzed using the Markov clustering algorithm to identify nodes that are highly interconnected within the miRNA-mediated gene expression regulatory network and are generally involved in the same functional modules or biological pathways.

TCGA miRNA/mRNA data sets

The expression profiles of miRNAs and mRNAs and clinical information for a cohort of 490 patients with primary PCa were retrieved from The Cancer Genome Atlas (TCGA, Provisional, http://cancergenome.nih.gov, Supplementary Table S6). A language package for R was used to perform data statistical analysis.

Survival analysis

Follow-up data of all patients with primary PCa were collected from TCGA. The overall survival was calculated from the date of surgery to the date of the last follow-up or death. The biochemical recurrence (BCR)-free survival was defined as the interval between the time of the initial surgery and the date of the first occurrence of detectable consecutive increases in PSA levels. The distant-metastasis-free survival was determined as the interval from the time of the initial surgery to the observation date of metastatic lesions.

Cell culture

Two human PCa cell lines, LNCaP and PC3, were purchased from the American Type Culture Collection (Manassas, VA, USA) and cultured in RPMI 1640 medium (HyClone, Los Angeles, CA, USA) supplemented with 10% fetal bovine serum (GIBCO/Invitrogen, Carlsbad, CA, USA), 2 mM L-glutamine, and antibiotics. A normal human prostate epithelial cell line (PREC) was purchased from Lonza Company and cultured in PrEGM Bullet kit (Lonza, Allendale, NJ, USA) with antibiotics. All cell lines were maintained at 37 °C in a humidified chamber supplemented with 5% CO_2.

Animals

All animal experiments were performed according to the guidelines of the Institute for Laboratory Animal Research at Guangzhou Medical University, Guangzhou, P.R. China. BALB/c nude mice (4–5-week-old males) were obtained from Guangdong Medical Laboratory Animal Center and were housed five per cage in wire-top cages with sawdust bedding in an isolated, clean, air-conditioned room at a temperature of 25–26 °C, a relative humidity of ~50% and with a 12 h light cycle/day.

Cellular transfection

Commercial miR-188-5p mimics (miR-188-mimic, Cat. No.: miR10005301-1-5), miR-193a-5p mimics (miR-193a-mimic, Cat. No.: miR10000459-1-5), miRNA mimic control (NC-mimic, Cat. No.: miR01101-1-5), miR-188-5p inhibitor (anti-miR-188, Cat. No.: miR20005301-1-5), miR-193a-5p inhibitor (anti-miR-193a, Cat. No.: miR20000459-1-5), and a nonspecific anti-miRNA control (anti-NC, Cat. No.: miR02201-1-5) were purchased from RiboBio (Guangzhou, China). The pCDNA3.1-UBE2i and pCDNA3.1-TP73 vectors were generated by cloning the ORFs of the *UBE2i* and *TP73* genes into the pCDNA3.1 vector, performed by HYYMed (Guangzhou, China), and the pCDNA3.1 backbone vector was used as a blank control vector. These vectors were transfected into PCa cells using Lipofectamine 2000 reagent (Invitrogen Life Technologies, Carlsbad, CA, USA) according to the manufacturer's protocol.

Generation of the in vivo xenograft model

LNCaP cells transfected with miR-188-5p/miR-193a-5p, miR-NC, anti-miR-188-5p/miR-193a-5p, or anti-NC lentivectors were used to construct the xenograft model of PCa for the in vivo tumor formation assay, as described in our previous studies[5,6]. Detailed information on model construction and tumor volume calculation is provided in Supplementary File S1—section 6.

Quantitative reverse transcription-PCR (qRT-PCR)

The qRT-PCR analyses for miRNAs and mRNAs in different cells were performed as described in our previous studies[5,6,31]. The primer sequences are listed in Supplementary Table S7.

Western blotting

Western blot analysis was performed as described in our previous studies[5,6,31]. Detailed information of the specific antibodies is provided in Supplementary Table S8.

Luciferase reporter assay

Luciferase reporter assay was performed to confirm direct binding efficiency of miRNAs and the corresponding target mRNA as described in our previous studies[5,6,31]. Detailed information is provided in Supplementary File S1—section 7.

Cell viability assay

Cell viability of PCa cells transfected with different vectors was detected with a Cell Counting Kit-8 (CCK-8, Cat No. C0037, Beyotime Biotechnology, Jiangsu, China) assay according to the protocol described in our previous studies[5,6,32].

Cell invasion and migration assays

The cell invasion and migration abilities of PCa cells transfected with different vectors were detected by the transwell and the scratch wound-healing motility assays, respectively, according to the protocol described in our previous studies[5,6,32].

Apoptosis assay

Cell apoptosis of PCa cells transfected with different vectors was detected using the APC-conjugated Annexin V (Annexin V-APC)/7-aminoactinomycin D (7-AAD) Kit (Cat. No.: LK-AP104-60, Multi Sciences (Lianke) Biotech Co., Ltd., Hangzhou, China) according to the protocol described in our previous studies[5,6,32].

Statistical analysis

SPSS version 13.0 for Windows (SPSS Inc., IL, USA) was used for all statistical analyses in this study. All assays were performed in triplicate. Continuous variables are expressed as the mean ± s.e.m. Differences in the qRT-PCR and western blot data for different groups were evaluated using the Wilcoxon signed-rank test. The associations between miRNA/mRNA expression and various clinicopathological features of PCa patients were confirmed by two biostatisticians with Fisher's exact test for any 2×2 tables and the Pearson χ^2-test for non-2×2 tables. A Kaplan–Meier curve was used for the survival analysis, and the Cox regression model was used for the univariate and multivariate analyses. The Spearman correlation was calculated between the expression levels of miRNAs and the corresponding target mRNAs in PCa tissues. Differences were considered significant when the p-value was <0.05.

Acknowledgements
This study was supported by the National Natural Science Foundation of China (No. 81303153, 81673834, 81641102, 81470983) & Beijing Nova program (Z1511000003150126), National Key Basic Research Program of China (2015CB553706), Science and Technology Project of Guangdong Province (2014A030304068, 2016A020215018), the Fundamental Research Funds for the Central public welfare research institutes (no.Z2017082&L2017018).

Author details
[1]Institute of Chinese Materia Medica, China Academy of Chinese Medical Sciences, Beijing 100700, China. [2]Department of Urology & Pathology, Massachusetts General Hospital and Harvard Medical School, Boston, MA 02114, USA. [3]Department of Urology, Guangdong Key Laboratory of Clinical Molecular Medicine and Diagnostics, Guangzhou First People's Hospital, Guangzhou Medical University, Guangzhou 510180, China. [4]Urology Key Laboratory of Guangdong Province, The First Affiliated Hospital of Guangzhou Medical University, Guangzhou Medical University, Guangzhou 510230, China

Conflict of interest
The authors declare that they have no conflict of interest.

Publisher's note
Springer Nature remains neutral with regard to jurisdictional claims in published maps and institutional affiliations.

Supplementary Information accompanies this paper at (https://doi.org/10.1038/s41419-018-0293-7).

Received: 18 September 2017 Revised: 6 December 2017 Accepted: 4 January 2018
Published online: 21 February 2018

References

1. Ferlay, J. et al. *Cancer Incidence and Mortality Worldwide: IARC CancerBase No. 11*. (International Agency for Research on Cancer, Lyon, France, 2013). GLOBOCAN 2012 v1.0.
2. Cheng, J. et al. The role of mesenchymal stem cells in promoting the transformation of androgen-dependent human prostate cancer cells into androgen-independent manner. *Sci. Rep.* **6**, 16993 (2016).
3. Shafi, A. A., Yen, A. E. & Weigel, N. L. Androgen receptors in hormone-dependent and castration-resistant prostate cancer. *Pharmacol. Ther.* **140**, 223–238 (2013).
4. He, H. C. et al. Global analysis of the differentially expressed miRNAs of prostate cancer in Chinese patients. *Bmc. Genom.* **14**, 757 (2013).
5. Cai, C. et al. miR-195 inhibits tumor progression by targeting RPS6KB1 in human prostate cancer. *Clin. Cancer Res.* **21**, 4922–4934 (2015).
6. Lin, Z. Y. et al. MicroRNA-224 inhibits progression of human prostate cancer by downregulating TRIB1. *Int. J. Cancer* **135**, 541–550 (2014).
7. Zhou, A., Molinaro, R. J., Malathi, K. & Silverman, R. H. Mapping of the human RNASEL promoter and expression in cancer and normal cells. *J. Interferon Cytokine Res.* **2**, 595–603 (2005).
8. Fesinmeyer, M. D., Kwon, E. M., Fu, R., Ostrander, E. A. & Stanford, J. L. Genetic variation in RNASEL and risk for prostate cancer in a population-based case-control study. *Prostate* **71**, 1538–1547 (2011).
9. Schoenfeld, J. D. et al. A single nucleotide polymorphism in inflammatory gene RNASEL predicts outcome after radiation therapy for localized prostate cancer. *Clin. Cancer Res.* **19**, 1612–1619 (2013).
10. Narayanan, T., Gersten, M., Subramaniam, S. & Grama, A. Modularity detection in protein-protein interaction networks. *BMC Res Notes* **4**, 569 (2011).
11. Weinstein, I. B. & Zhou, P. In *Encyclopedia of Cancer* vol. 1 (ed. Bertino, J. R.) 256–267 (Academic Press, New York, 1996).
12. Lu, J. W. et al. Clinical implications of deregulated CDK4 and Cyclin D1 expression in patients with human prostate cancer. *Med. Oncol.* **30**, 379 (2013).
13. Nakamura, Y. et al. Cyclin D1 (CCND1) expression is involved in estrogen receptor beta (ERβ) in human prostate cancer. *Prostate* **73**, 590–595 (2013).

14. Sherr, C. J. Mammalian G1 cyclins and cell cycle progression. *Proc. Assoc. Am. Physicians* **107**, 181–186 (1995).
15. Yang, A. & McKeon, F. P63 and P73: P53 mimics, menaces and more. *Nat. Rev. Mol. Cell Biol.* **1**, 199–207 (2000).
16. Yang, A., Kaghad, M., Caput, D. & McKeon, F. On the shoulders of giants: p63, p73 and the rise of p53. *Trends Genet.* **18**, 90–95 (2002).
17. McKeon, F. D. p63 and p73 in tumor suppression and promotion. *Cancer Res Treat.* **36**, 6–12 (2004).
18. Guan, M. & Chen, Y. Aberrant expression of DeltaNp73 in benign and malignant tumours of the prostate: correlation with Gleason score. *J. Clin. Pathol.* **58**, 1175–1179 (2005).
19. Al-Haj, L., Blackshear, P. J. & Khabar, K. S. Regulation of p21/CIP1/WAF-1 mediated cell-cycle arrest by RNase L and tristetraprolin, and involvement of AU-rich elements. *Nucleic Acids Res.* **40**, 7739–7752 (2012).
20. Shen, Z., Pardington-Purtymun, P. E., Comeaux, J. C., Moyzis, R. K. & Chen, D. J. Associations of UBE2I with RAD52, UBL1, p53, and RAD51 proteins in a yeast two-hybrid system. *Genomics* **37**, 183–186 (1996).
21. Chen, J. et al. Pathologically decreased expression of miR-193a contributes to metastasis by targeting WT1-E-cadherin axis in non-small cell lung cancers. *J. Exp. Clin. Cancer Res.* **35**, 173 (2016).
22. Yu, T. et al. MicroRNA-193a-3p and -5p suppress the metastasis of human non-small-cell lung cancer by downregulating the ERBB4/PIK3R3/mTOR/S6K2 signaling pathway. *Oncogene* **34**, 413–423 (2015).
23. Zhang, P. et al. Downregulation of miR-193a-5p correlates with lymph node metastasis and poor prognosis in colorectal cancer. *World J. Gastroenterol.* **20**, 12241–12248 (2014).
24. Lin, C. H. et al. MiR-193a-5p/ERBB2 act as concurrent chemoradiation therapy response indicator of esophageal squamous cell carcinoma. *Oncotarget* **7**, 39680–39693 (2016).
25. Jacques, C. et al. miRNA-193a-5p repression of p73 controls Cisplatin chemoresistance in primary bone tumors. *Oncotarget* **7**, 54503–54514 (2016).
26. Wang, L. & Liu, H. microRNA-188 is downregulated in oral squamous cell carcinoma and inhibits proliferation and invasion by targeting SIX1. *Tumour Biol.* **37**, 4105–4113 (2016).
27. Fang, F. et al. MicroRNA-188-5p suppresses tumor cell proliferation and metastasis by directly targeting FGF5 in hepatocellular carcinoma. *J. Hepatol.* **63**, 874–885 (2015).
28. Zhang, H. et al. miR-188-5p inhibits tumour growth and metastasis in prostate cancer by repressing LAPTM4B expression. *Oncotarget* **6**, 6092–6104 (2015).
29. Yu, H., Kim, P. M., Sprecher, E., Trifonov, V. & Gerstein, M. The importance of bottlenecks in protein networks: Correlation with gene essentiality and expression dynamics. *PLoS Comput. Biol.* **3**, e59 (2007).
30. Alvarez-Cubero, M. J. et al. Association between RNASEL, MSR1, and ELAC2 single nucleotide polymorphisms and gene expression in prostate cancer risk. *Urol. Oncol.* **34**, 431.e1–8 (2016).
31. Zhang, Y. et al. Comprehensive analysis of microRNA-regulated protein interaction network reveals the tumor suppressive role of microRNA-149 in human prostate cancer via targeting AKT-mTOR pathway. *Mol. Cancer* **13**, 253 (2014).
32. Chen, G. et al. CC chemokine ligand 18 correlates with malignant progression of prostate cancer. *Biomed. Res Int.* **2014**, 230183 (2014).